Proteomic Identification of Pterostilbene-Mediated Anticancer Activities in HepG2 Cells

ARTICLE *in* CHEMICAL RESEARCH IN TOXICOLOGY · JUNE 2014

Impact Factor: 3.53 · DOI: 10.1021/tx5001392 · Source: PubMed

Chemical Research in Toxicology

Article

pubs.acs.org/crt

Proteomic Identification of Pterostilbene-Mediated Anticancer Activities in HepG2 Cells

N. Suganya,[†] E. Bhakkiyalakshmi,[†] T. S. Subin,[‡] K. Krishnamurthi,[‡] S. Saravana Devi,[‡] K. Lau,[§] T. V. Sekar,[§] R. Paulmurugan,[§] and K. M. Ramkumar*[,†]

[†]SRM Research Institute, SRM University, Kattankulathur, Tamilnadu, India

[‡]Environmental Health Division, National Environmental Engineering Research Institute, Nagpur, India

[§]Department of Radiology, Stanford University School of Medicine, 3155 Porter Drive, Stanford, California 94305, United States

Supporting Information

ABSTRACT: In the present study, we attempt to shed light on the underlying molecular mechanism of the anticancer activity of pterostilbene (PTS) in HepG2 cells through the proteomic approach. PTS was found to induce apoptosis by altering the expression of apoptotic genes and the G2/M phase of cell cycle arrest. Further, the 2-DE map showed the expression of 72 differentially regulated proteins in PTS-treated HepG2 cells, of which 8 spots with >2 fold up- or down-regulated level were identified by MALDI-TOF analysis, which has a regulatory role in apoptosis. These findings for the first time offer valuable insights into the mechanism of apoptotis by PTS in HepG2 cells.

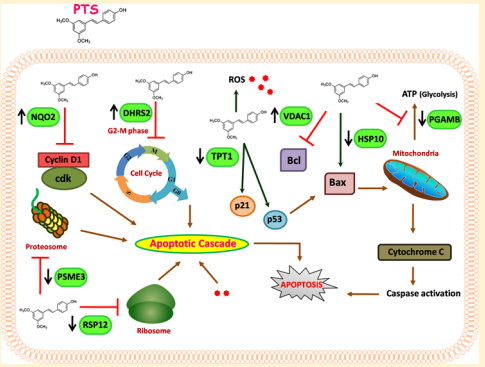

INTRODUCTION

Preclinical and epidemiological studies support that polyphenols from the natural sources possess a wide range of cancer chemopreventive properties. One such natural phytoalexin is pterostilbene (PTS), which belongs to the stilbene group of polyphenol, widely distributed in blueberries and grapes.[1] It is well known for its antioxidant activity and increased oral bioavailability.[2,3] It has also been reported to have diverse pharmacologic activities including anticancer effects in various animal models.[4]

PTS has been demonstrated to induce growth arrest and apoptosis in various cancer cell lines through the activation of mitochondrial caspase pathway, increased nucleosome release, cell cycle arrest, and DNA damage by modifying cell cycle-regulating proteins such as cyclin.[2,4,5] It is also accounted for its role in down regulating the inflammatory gene expression by inhibiting multiple signaling pathways including NF-κB and AP-1.[6]

Further, PTS has been shown to inhibit the metastatic potential of tumor cells by suppressing colony formation, tumor cell migration, invasion, and angiogenesis.[6] It has been reported to decrease the levels of growth factors involved in neoangiogenesis in hepatocellular carcinomas by modulating the drug metabolizing enzymes, thereby either preventing the activation of protooncogenes or detoxifying the carcinogens.[7] Even though PTS has been reported for its apoptotic property, the exact mechanism of its action has not been clearly defined. Hence, a detailed investigation is necessary to contour the molecular mechanism by which PTS triggers cancer cell apoptosis.

Global proteomics has been successfully employed to identify cancer specific protein markers and hence paves the way to a new area of cancer chemotherapy and early detection. Proteomics aims to investigate protein expression profile in specific diseased conditions and has been reported by many investigators in various cancer cell lines.[8,9] With relevance to these earlier reports, in this study we aimed at screening differentially regulated proteins by PTS in HepG2 cells (human hepatocellular liver carcinoma cell line) using a proteomic approach. Our data revealed that PTS-induced apoptosis in HepG2 cells with the modulation of various apoptosis related proteins such as VDAC1 (voltage-dependent anion-selective channel protein1), NQO2 (NAD(P)H dehydrogenase, quinone 2), DHRS2 (dehydrogenase (reductase) SDR family member 2), etc. and further confirmed by quantitative real-time polymerase chain reaction (q-RT-PCR). These findings from this study will set a strong platform to reveal the molecular mechanism behind PTS action in cancer cell death.

EXPERIMENTAL PROCEDURES

Chemicals. Pterostilbene was purchased from Sigma-Aldrich (St. Louis, MO). A 50 mM stock of PTS was prepared in dimethyl sulfoxide (DMSO) and kept frozen at −20 °C.

Received: April 15, 2014

   dx.doi.org/10.1021/tx5001392 | *Chem. Res. Toxicol.* XXXX, XXX, XXX−XXX

Table 1. q-RT-PCR Primer Sequences for Validated Targets

gene name	abbreviated name	forward primer 5′-3′	reverse primer 5′-3′
dehydrogenase (reductase) SDR family member 2	DHRS2	TGGGTCTCACTAGAACAC	CAGGAAGGACACGATTCC
NAD(P)H dehydrogenase, quinone 2	NQO2	GAGTGGAAACCCACGAAG	AGCAAACCGGAATCGTAG
voltage-dependent anion-selective channel protein 1	VDAC1	TCAATCTTGCCTGGACAG	TCCTAGACCAAGCTTGTG
B-cell lymphoma 2	BCl-2	GCTGAGGCAGAAGGGTTATG	GCCCCCTTGAAAAAGTTCAT
Bcl-2 associated X protein	BAX	AGGGTTTCATCCAGGATCGAGCAG	ATCTTCTTCCAGATGGTGAGCGAG
caspase 3	CASP3	TTTGTTTGTGTGCTTCTGAGCC	ATTCTGTTGCCACCTTTCGG
actin-β	ACT	GGCGGACTATGACTTAGTTG	AAACAACAATGTGCAATCAA

Cell Culture Conditions. HepG2 cells (human hepatocellular liver carcinoma cell line) were grown in Dulbecco's modified Eagle's medium (Gibco, USA) supplemented with 10% heat-inactivated fetal bovine serum (FBS, Gibco, USA) and 1% penicillin/streptomycin at 37 °C in an atmosphere containing 5% CO_2.

Cytotoxicity Assay. Cytotoxicity was assessed using the MTT (3-(4,5-dimethylthiazol-2-yl)-2,5-diphenyl tetrazolium bromide) assay. HepG2 cells (1×10^4 cells/well) were seeded and grown overnight in 96-well plates and then treated with different concentrations of PTS (0−100 μM). Control cells were treated with DMSO (0.2%). After 0−48 h of incubation, 10 μL of MTT solution (5 mg/mL) was added to each well, and plates were incubated at 37 °C for 4 h. Then the formazan crystals formed by mitochondrial reduction of MTT were solubilized in DMSO (150 μL/well), and the absorbance was read at 570 nm using a Microplate Reader (BioRad, USA). Percent inhibition of cytotoxicity was calculated as a fraction of control (without PTS) and expressed as percentage of cell viability. Each experiment was performed in triplicate.

Isolation and Culturing of Primary Rat Hepatocytes. Hepatocytes from male Wistar rats (150 to 200 g) were prepared by an EDTA *in situ* perfusion method as described earlier.[10] Briefly, the cell pellets were resuspended in DMEM low glucose containing 10% fetal calf serum and 1% penicillin and streptomycin. Cell viability was assessed by the trypan blue exclusion test, and the isolated hepatocytes were seeded on collagen-coated multiwell plates and left for 3 h to attach at 37 °C in a humidified atmosphere of 5% CO_2 in air. The culture medium was replaced with fresh serum free DMEM medium to which 10 μL aliquots of various concentrations of PTS (0 to 100 μM) prepared in DMSO were added and incubated for 24 h. Control cells were treated with equal volumes of DMSO as a vehicle. Final DMSO concentration was 0.2% for all treatments. After the experimental period, the cells were incubated with 10 μL of MTT solution (5 mg/mL) for 4 h. Subsequently, the medium was aspirated, and the formazan crystals were solubilized by adding DMSO (150 μL/well). The absorbance was measured at 570 nm using a microplate reader (BioRad, USA). Cell viability was expressed as the percentage of viable cells under each treatment regimen.

Measurement of Intracellular Reactive Oxygen Species (ROS). Intracellular ROS levels were measured using an oxidation-sensitive fluorescent dye, 2,7-dichlorodihydrofluorescein diacetate (H2DCFDA). Briefly, 24 h after initial plating, HepG2 cells (5×10^6 cells/well) in 6-well plates were treated with PTS (0−50 μM) for 24 h, H2DCFDA (20 μM) was added to the cells and further incubated for 30 min at 37 °C. Then the cells were trypsinized for 2 min, and the reaction was stopped with phosphate-buffered saline (PBS) containing 10% fetal calf serum (FCS). Live cells were pelleted by centrifugation (800*g*, 10 min), washed, and resuspended in PBS. The resultant fluorescence intensity was measured by flow cytometry at 492 nm excitation wavelength, 527 nm emission wavelength, and 517 nm cutoff wavelength (BD FACS Calibur, Becton Dickinson, USA). The fluorescence intensity was directly proportional to the amount of free radicals produced by the cells.

Measurement of Mitochondrial Membrane Potential. Mitochondrial membrane potential was measured by the incorporation of a cationic fluorescent dye rhodamine 123 as described by Zhang and Zhao.[11] Briefly, after 24 h incubation of HepG2 cells (5×10^6 cells/well) in 6-well plates with PTS (0−50 μM), the cells were changed to serum-free medium containing rhodamine 123 (5 μM) and incubated for 15 min at 37 °C. The cells were then collected, and the florescence intensity was analyzed within 15 min by a spectrofluorimeter (Varian-Cary Eclipse; 490 nm excitation and 515 nm emission).

Cell Cycle Analysis. Quantitative cell cycle analysis was performed using propidium iodide with a FACSVantage SE flow cytometer (Becton Dickinson, USA). For the determination of the cell cycle phases, a peak area of FL2-H was recorded on a linear scale. The percentage of cells in sub-G1, G1, S, and G2/M phases were determined using CELLQuest Software (Becton Dickinson, USA). The cells (1×10^6 cells/well) in 6-well plates were treated with PTS (0−50 μM) for 24 h and harvested by centrifugation at 1000*g* for 5 min at 4 °C. Pellets were rinsed with ice cold phosphate-buffered saline (PBS) and fixed with ice cold 70% ethanol for 2 h. Cells were then washed once with PBS and stained with staining buffer (PBS containing 40 μg/mL of propidium iodide, 100 μg/mL RNase A, and 0.1% Triton X-100) for 15 min at 37 °C in the dark. The cells incubated in DMEM only were used as the control. For flow cytometry analysis duplicate samples were used for each treatment, and each experiment was repeated at least three times. Approximately, 10,000 cells were evaluated for each sample. In all flowcytometric determinations, cell debris and cell clumps were excluded from the analysis by suitable gating. The effect of PTS on apoptosis was determined by the changes in the proportion of different phases of the cells.

Quantitative Real Time Polymerase Chain Reaction (q-RT-PCR). A variety of q-RT-PCR primers were designed based on the NCBI human mRNA and genomic DNA sequence database. DNA fragments of PCR products were designed within 200 bp amplification length. Forward and reverse primers were primarily designed from different exons to decrease the background noise from genomic DNA contamination. Primer sequences are listed in Table 1. HepG2 cells were treated with 10, 25, and 50 μM PTS for 24 h and q-RT-PCR was performed following the manufacturers' protocol. Briefly, each reaction contained 2 μL of cDNA (0.1 μg of RNA equivalent), 0.8 μL of primers (containing 100 pM of forward and reverse primers), 2.2 μL of H_2O, and 5 μL of Sofast EvaGreen supermix. q-RT-PCR was performed in an Eppendorf thermocycler with a three-step program (95 °C for 30 s, 55 °C for 30 s, and 72 °C for 45 s for 50 cycles). q-RT-PCR data were analyzed by software. Gene expression fold change was obtained by dividing the treated group signal by that of the base expression level signal of the corresponding gene in untreated cells. The results were normalized using the q-RT-PCR signal from the β-actin of respective samples.

Protein Extraction and Quantification. HepG2 cells were treated with 50 μM PTS for 24 h, and the cells were collected, washed by precooled PBS three times, centrifuged again, resuspended in 100−200 μL of lysis buffer and kept in a shaker at 4 °C for 1 h, then lysed by sonication, and then centrifuged to collect the supernatant. The proteins were quantified using 2-D Quant Kit (GE Healthcare, USA) according to the manufacturer's instructions.

Two-Dimensional Gel Electrophoresis (2-DE), Staining, and Image Analysis. The cell lysate prepared from PTS treated and control cells were used for 2-DE according to the manufacturer's instructions (Bio-Rad, USA). The isoelectric focusing (IEF) was performed on precast 17 cm immobilized pH 4−7 gradient (IPG) strips using a Protein IEF cell (Bio-Rad, USA). One hundred

dx.doi.org/10.1021/tx5001392 | *Chem. Res. Toxicol.* XXXX, XXX, XXX−XXX

micrograms of the protein sample was mixed with rehydration buffer, and the solubilized sample was loaded onto an IPG strip through passive in-gel rehydration overnight. After rehydration, IEF was carried out using the following conditions: 20 min at 250 V, 5 h at 250–40,000 V increasing at the rate of 10,000 V/h, and then held at 500 V for 15 min. After IEF, the gel strips were equilibrated in equilibration buffer-I solution for 10 min, followed by further incubation in equilibration buffer-II for an additional 10 min.

The equilibrated strip was subjected to sodium dodecyl sulfate–polyacrylamide gel electrophoresis (SDS–PAGE) on 12% acrylamide gels. The strip was sealed at the top of the 1.0 mm thick second-dimensional gel with the help of 0.5% low-melting agarose in stacking buffer. Gels were run at a constant voltage of 60 V for 20 min and then 250 V until the bromophenol blue front reached the lower edge of the cassette. The gel was removed from the cassette and placed in the fixative solution overnight. Then the gel was soaked in 0.02% sodium thiosulfate solution for 1 min. Again, the gel was washed with distilled water and placed in silver nitrate solution for 20 min on the shaker. Before placing the gel in developing solution, the gel was washed with distilled water for 1 min. The developing process was continued until the appearance of protein spots. Finally, the staining was terminated by stop solution.

Image Analysis. The stained analytical gels were scanned by a gel documentation system (Bio-Rad, USA), and the image analysis including image editing, spot finding, quantitation, and matching was carried out using the two-dimensional analysis software package Delta2D 3.6/DECODON (DECODON GmbH, BioTechnikum Greifswald, Germany). The software was used to calculate the spot intensity by integrating the optical density over the spot area. A reference gel was selected at random from the gels of the control group for each experiment, and detected spots from the other gels in the control data set were matched to those in the selected reference gel. The relative OD and relative volume were also calculated in order to correct for differences in gel staining. Each spot intensity volume was processed by background subtraction and total spot volume normalization; the resulting spot volume percentage was used for comparison.

MS-MS Analysis of Tryptic Peptides. Excised protein spots were destained with destaining solution (30 mM potassium ferricyanide and 100 mM sodium thiosulfate) with shaking for 5 min. After removal of the solution, gel pieces were washed with water and followed by 50 mM ammonium bicarbonate and 50% acetonitrile for 30 min. The gel pieces were then dehydrated with 100% acetonitrile and dried in a speedvac. The dried gel pieces were rehydrated with 20 to 40 μL of 50 mM ammonium bicarbonate containing 20 ng of trypsin (Promega, USA) and incubated overnight at 37 °C. The subsequent tryptic digests were desalted using Millipore C18 ziptip and then eluted with the matrix (alpha-cyano-4-hydroxycinnamic acid from Agilent) for MALDI-TOF/TOF analysis. Protein identification was done by searching MS/MS spectra of a subset of peptides against the Swiss-Prot database using the MASCOT search engine.

Statistical Analysis. All data were expressed as the mean ± SEM of number of experiments (n = 3). The data for various parameters were tested by ANOVA using SPSS, version 7.5 (SPSS Inc., USA), and the group means were compared by Duncan's multiple range test. Values were considered statistically significant with $p < 0.05$.

RESULTS

Cytotoxic Effect of PTS in HepG2 Cells. To determine the cytotoxic effect of PTS, HepG2 cells treated with different concentrations of PTS for various time intervals were assessed by the MTT assay. For the dose-dependent study, the cells were treated with different PTS concentrations (0–100 μM) for 24 h. The results showed that PTS effectively inhibits the viability of HepG2 cells in a dose-dependent manner with an IC_{50} value at around 60 μM (Figure 1). Time-dependent cytotoxic effect was carried out with 10, 25, and 50 μM concentrations of PTS for up to 48 h. PTS showed significant

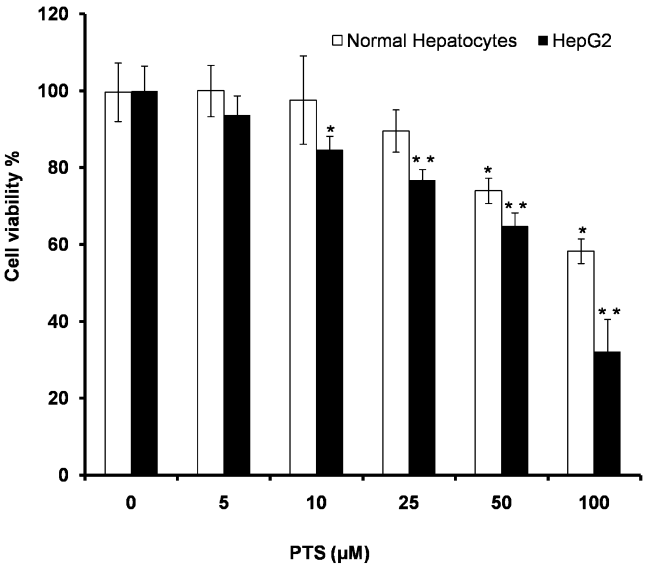

Figure 1. Cytotoxicity of PTS in HepG2 cells. Cells were treated with different concentrations of PTS for 24 h, and cell viability was determined by the MTT assay. Data are represented as the mean ± SEM of three independent experiments (*$p < 0.05$; **$p < 0.001$).

cytotoxic effect at all the time points studied when compared to the control cells. The percentage of inhibition was found to be increased significantly with the increase in exposure time (Figure 2).

In order to study the cytotoxicity of PTS on normal cells, we have taken primary rat hepatocytes, and the toxicity was evaluated by the MTT assay. With different PTS concentrations (0–100 μM), the cytotoxicity of normal hepatocytes was found to be minimal when compared to HepG2 cells.

Effect of PTS on Free Radical Generation. In order to elucidate the role of PTS in inducing free radical generation, HepG2 cells were treated with different concentrations of PTS (0–50 μM) for 24 h and subjected to H2DCFDA-fluorescence analysis. Flow cytometric analysis showed a concentration-dependent increase in the free radical generation as assessed by changes in the fluorescence shift (Figure 3A). The result indicates that PTS induces free radical generation, which may be involved in the induction of apoptosis.

Effect of PTS on Mitochondrial Membrane Potential. To investigate whether the apoptosis induced by PTS in HepG2 cells involved the loss of mitochondrial integrity, the mitochondrial membrane potential was analyzed. The HepG2 cells were exposed to different concentrations of PTS (0–50 μM) for 24 h and incubated with rhodamine 123 for 15 min. The fluorescent intensity of rhodamine 123 is inversely proportional to the mitochondrial membrane potential. The untreated control groups of HepG2 cells showed strong fluorescence by spectrofluorimetry. In contrast, PTS treatment induced the fall of the fluorescent signal in a concentration-dependent manner (Figure 3B). The result indicates that PTS induces changes in mitochondrial membrane potential, which may be involved in the mitochondria-mediated cell death.

Cell Cycle Arrest Induced by PTS. To examine the effect of PTS on the cell cycle, HepG2 cells were treated with different concentrations of PTS (0–50 μM) for 24 h and analyzed by flow cytometry using propidium iodide. The results showed a dose-dependent G2/M arrest in the cell cycle in PTS-

dx.doi.org/10.1021/tx5001392 | Chem. Res. Toxicol. XXXX, XXX, XXX–XXX

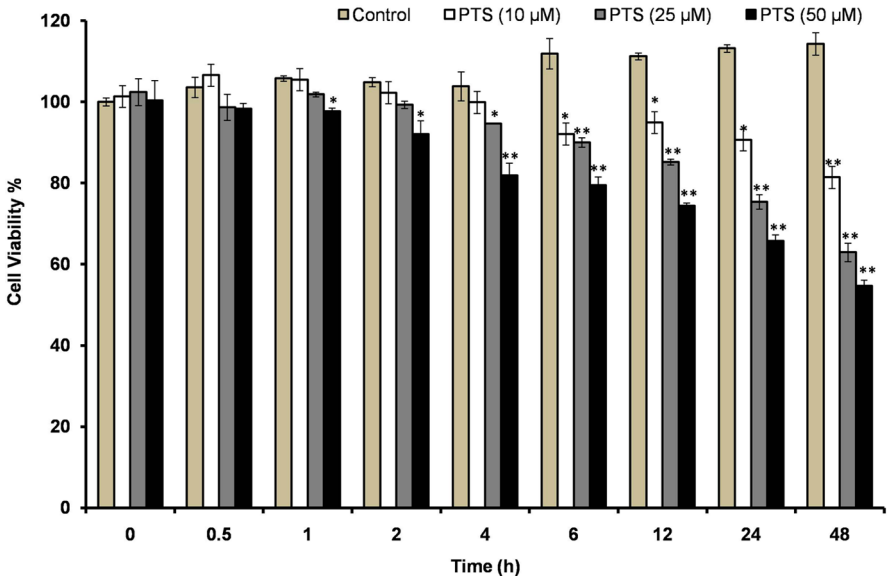

Figure 2. Time-dependent inhibitory effect of PTS on the cell viability of HepG2. Cells were treated with different concentrations of PTS for 0−48 h, and the inhibitory effect was determined by the MTT assay. Data are represented as the mean ± SEM of three independent experiments (*p < 0.05; **p < 0.001).

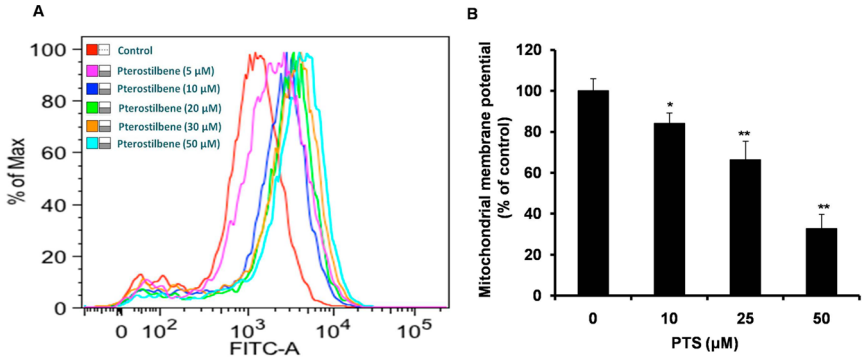

Figure 3. Effect of PTS on free radical production assessed by flowcytometric analysis using H2DCFDA (A) and mitochondrial membrane potential using rhodamine 123 (B) in HepG2 cells. Cells were treated with different concentrations of PTS for 24 h and incubated with H2DCFDA and detected for free radical generation using a flow cytometer. For mitochondrial membrane potential, the cells were stained with rhodamine 123, and then fluorescence intensity was measured using spectrofluorimetry. The fluorescent signal of control is represented as 100%, and the experimental data are expressed as changes in the percentage in a histogram. Data are represented as the mean ± SEM of three independent experiments (*p < 0.05; **p < 0.001).

treated cells and a marked raise of about 81.3% of G2/M phase cells was observed at the dose of 50 μM (Figure 4).

mRNA Expression of Apoptotic Genes. The mRNA expression levels of pro-apoptotic gene Bax, caspase-3, and antiapoptotic gene Bcl-2 in HepG2 cells treated with PTS were assessed by q-RT-PCR. The results showed a significant increase in mRNA expression of Bax and significant decrease of Bcl-2. The ratio of Bax/Bcl-2 shows a consistent increase from the cells treated with PTS. In addition, the increase in the expression levels of caspase-3 mRNA was also observed. (Figure 5).

Modulation in Protein Profile Analyzed Using 2-DE. To examine the modulation in protein profile after PTS treatment in HepG2 cells, 2-DE was carried out, and images of control and PTS-treated (50 μM) samples are presented in Figure 6. Image spots in 2-D gels were initially detected and matched with the control. The intensity volume of each spot was processed by background subtraction and total spot volume normalization, and the resulting spot volume in relative percentage was used for comparison. The spots with significant up- or down-regulated level of protein between the PTS-treated samples with the control were considered for further analysis.

Among 72 spots observed by 2-DE in the control and treated cells, 26 spots were identified to be differentially regulated (up-regulation, 6 ± 1 fold, 4 spots; down-regulation, 2 ± 1 fold, 22 spots), out of which 8 spots confirmed by MALDI-TOF analysis showed significant regulation (2 ± 1 fold compared to the respective spot from the control sample) and consistent expression (Supporting Information, Figure S1 and Table S1). These spots were recognized as VDAC1, NQO2, DHRS2, HSP10 (heat shock protein10), RPS12 (40S ribosomal protein S12), PGAM-B (phosphoglycerate mutase B), PSME-3 (proteosome activator complex subunit 3), and TPT1 (translationally controlled tumor protein) proteins (Table 2).

Out of 8 proteins, 3 were found to be up-regulated (NQO2, VDAC1, DHRS2), and 5 were down-regulated (HSP10, RPS12, PGAM-B, PSME-3, and TPT1) in the PTS-treated cells, and the order of magnitude of the changes differs widely

dx.doi.org/10.1021/tx5001392 | Chem. Res. Toxicol. XXXX, XXX, XXX−XXX

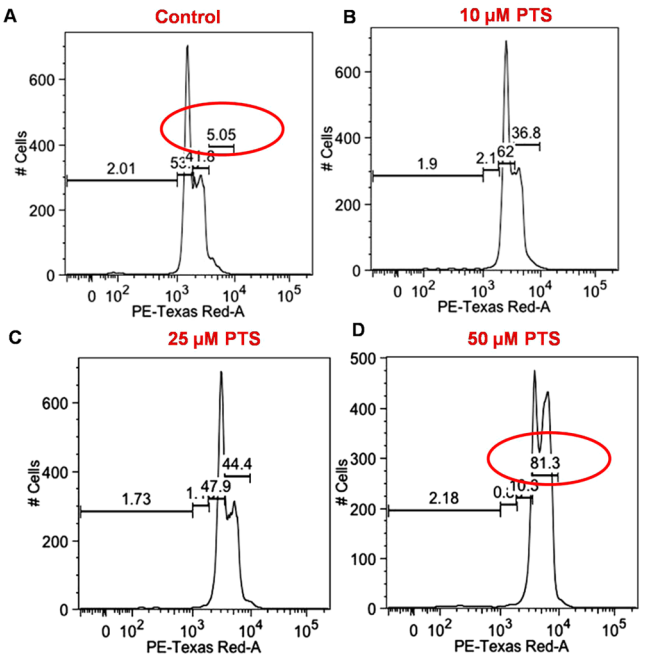

Figure 4. PTS-induced cell cycle arrest and apoptosis in HepG2. Cells were treated with different concentrations of PTS and stained with propidium iodide, and the distribution of the cells in different phases was determined by flow cytometry. (A) 0 μM; (B) 10 μM; (C) 25 μM; and (D) 50 μM PTS.

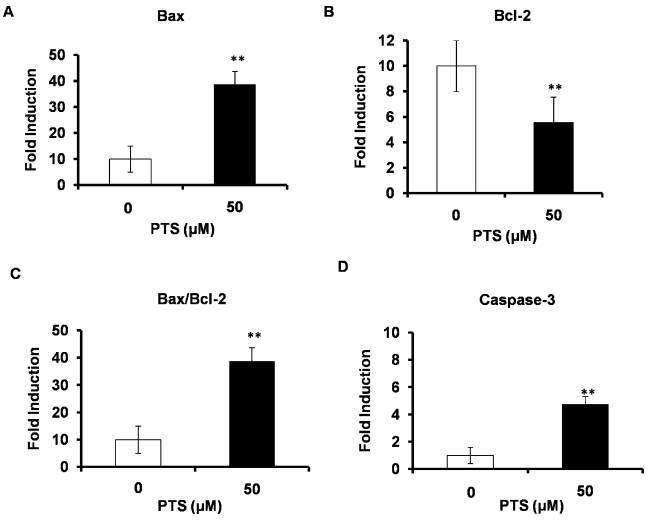

Figure 5. Quantitative real-time PCR analysis. mRNA expression levels of pro-apoptotic and antiapoptotic proteins in HepG2 cells treated with PTS of 50 μM. (A) Bax; (B) Bcl-2; (C) Bax/Bcl-2; and (D) caspase-3. Data are represented as the mean ± SEM of three independent experiments (*$p < 0.05$; **$p < 0.001$).

when compared with the control cells. After PTS treatment, the proteins NQO2, VDAC1, and DHRS2 showed significant up-regulation to a fold of 6.4, 3.24, and 5.75 compared with the control cells. Among the up-regulated proteins, the magnitude was found to be very high in NQO2 protein. The level of HSP10 protein was decreased in the PTS-treated cells with about 3.32 fold when compared with the control cells. Also the other proteins PGAM-B, PSME-3, and TPT1 showed fold decreases of 2.6, 1.83, and 1.56 (Table 2).

To characterize the mRNA expression of the differentially regulated proteins, DHRS2, NQO2, and VDAC1 were chosen for further analysis by quantitative real-time PCR. The expression profiles of these genes after PTS treatment are shown in Figure 7. The DHRS2 and NQO2 transcriptions increased significantly to 1.8 and 2.2 fold higher, respectively. No statistically significant change was detected for VDAC1 protein at lower concentrations. The up-regulated tendency of the three selected genes at transcription levels obtained from real-time PCR was consistent with the 2-DE data.

DISCUSSION

Numerous natural compounds show potential health benefits and proved to act against a wide range of diseases including cancer. The properties of natural compounds showing an effective role against tumor initiation, promotion, and progression, angiogenesis, and metastasis suppression in various carcinomas make them an attractive basis for identifying effective anticancer agents.[12] Among various agents, different polyphenols were effectively evidenced to have pharmacological, putative anticancer properties and act against different types of cancers.[13] Some polyphenols have been shown to reduce the levels of specific proteins in various cancer cell lines, which are considered as biomarkers for therapeutic evaluation and are well documented by many *in vitro* and *in vivo* models suggesting that polyphenols hinder the consequences of cancer.[14] For their vital role as chemopreventing agents, a few polyphenols like curcumin, hesperetin, quercetin, resveratol, and gallic acid have been approved by the Food and Drug Administration (FDA), and a few other compounds are in clinical trials.

Accumulating evidence supports the effect of polyphenols against numerous cancerous conditions.[15] In the present study, PTS showed dose- and time-dependent cytotoxic effect on HepG2 cells with an IC_{50} of 60 μM. This finding coincides with the previous findings of Mannal et al. on the cytotoxicity of PTS on pancreatic cancer cells.[16]

The increased free radical generation plays a vital role in the induction of cancer cell apoptosis. ROS may provide a unique opportunity to target the cancer cells as it damages the cellular components like DNA, protein, and lipid membranes.[17] Our results demonstrated that the PTS treatment increased the intracellular ROS generation and causes severe oxidative stress-mediated cell death. The change in ROS signal after 24 h of treatment with different concentrations of PTS increased free radical generation, which was visualized by the shift in the DCF-fluorescent peak compared to that of the control. This result proves that altered ROS balance in the cell resulted in cell death. This finding was supported by previous reports, which showed the elevation of ROS in HepG2 cells after quercetin treatment exhausted the antioxidant defenses leading to cell death.[18] The changes induced in the mitochondrial membrane potential have been known to represent a determinant in the execution of cell death.[19] In the present study, we analyzed the effect of PTS on the mitochondrial membrane potential, and rhodamine 123 was used to detect changes in mitochondrial function since fluorescence of the dye decreases as mitochondrial membrane potential collapses. As shown in Figure 4, the percentage of rhodamine 123 was decreased significantly, which indicates that the PTS-induced apoptosis in HepG2 cells was mediated by a mitochondrial pathway and this loss of mitochondrial membrane potential correlated well with increased cell death.

dx.doi.org/10.1021/tx5001392 | *Chem. Res. Toxicol.* XXXX, XXX, XXX–XXX

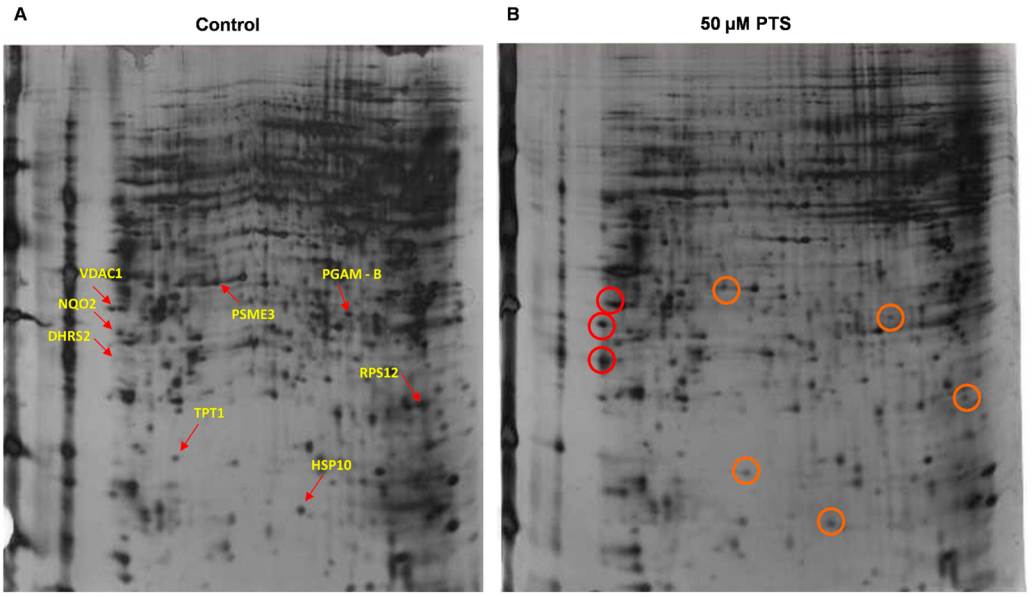

Figure 6. 2-DE maps of HepG2 control and PTS-treated HepG2 cells. The control cells (A) and HepG2 cells treated with 50 μM PTS (B) for 24 h were stained with silver nitrate. Protein spots marked on the maps were considered differentially expressed and identified by MALDI-TOF. These results are representative of three independent experiments.

Table 2. MALDI-TOF Analysis of Differentially Regulated Proteins in PTS-Treated HepG2 Cells

S. no.	abbreviation	protein description	accession number	theoretical molecular mass (kDa)	experimental molecular mass (kDa)	fold change
1	PGAM-B	phosphoglycerate mutase B	P18669	28.8	28.5	−2.6
2	RPS12	40S Ribosomal protein S12	Q76M58	14.9	24	−3.86
3	VDAC 1	voltage-dependent anion-selective channel protein 1	P46274	31	29.8	+3.24
4	NQO2	NAD(P)H dehydrogenase, quinone 2	AAH06096	25.9	26.2	+6.4
5	DHRS2	dehydrogenase (reductase) SDR family member 2	NP_005785	28	25.5	+5.75
6	HSP10	heat shock protein 10	NP_002148	10	9.8	−3.32
7	PSME-3	proteosome activator complex subunit 3	P61289	29.6	31	−1.83
8	TPT1	translationally controlled tumor protein	P13693	19.7	19.2	−1.56

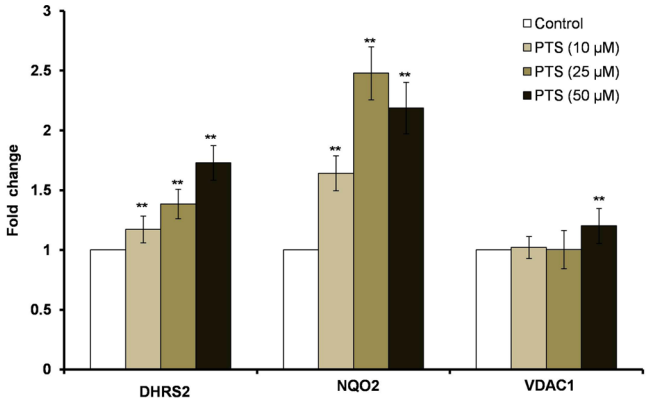

Figure 7. Quantitative real-time PCR analysis. mRNA expression levels of DHRS2, NQO2, and VDAC1 in HepG2 cells treated with different concentrations of PTS. Data are represented as the mean ± SEM of three independent experiments (*p < 0.05; **p < 0.001).

PTS induces cancer cell apoptosis by involving both caspase-dependent and -independent pathways.[20,21] PTS is also known to activate extracellular signal-regulated kinase 1/2, p38 mitogen-activated protein kinase, c-Jun N-terminal kinases 1/2, phosphatidylinositol 3-kinase/Akt, and protein kinase C whereby it inhibits nuclear factor κB (NF-κB) and activator protein-1 (AP-1)-dependent transcriptional activity.[22] PTS selectively inhibits mitogen-activated protein kinase and cyclin-dependent kinase induction through p53 activation, which plays a vital role in the regulation of cell cycle progression and triggers G0/G1, S, and G2/M phases of cell cycle arrest.[23]

The organic extract from a natural plant source containing quercetin glycosides, chlorogenic acid shows inhibition of the growth of HepG2 cells through cell cycle arrest in the G2/M phase.[24] Lee et al. showed that curcumin induces both G1/S and G2/M phases of cell cycle arrest in human osteosarcoma cells through DNA damage and decreases the level of cell cycle regulatory molecules.[25] Gallic acid, resveratol, xanthatin, eupatilin, and many flavonoids were reported to arrest the cell cycle at the G2/M phase in various cancer cells.[26] In this present study with HepG2 cells, PTS shows significant cell cycle arrest at the G2/M phase with a concentration of 50 μM for 24 h. Moreover, Patrick et al. demonstrated that the cell cycle arrest of PTS depends on its concentration and cell type.[16]

Effective strategies in tumor therapy are necessary to identify the differentially expressed proteins in tumor cells to retrieve the molecular mechanism behind the anticancer effect.[27]

dx.doi.org/10.1021/tx5001392 | Chem. Res. Toxicol. XXXX, XXX, XXX−XXX

Hence, in this study we attempted to find the proteins modulated in HepG2 cells after PTS treatment using 2-DE. A total of 72 spots were identified in the 2-DE map, which were either up- or down-regulated in PTS-treated cells when compared to control cells. Among these, 26 spots were differentially regulated, of which 8 spots showed 2 to 3 fold higher or lower expression than the respective spots in the control identified by MALDI-TOF analysis. Significant upregulation of VDAC1, NQO2, and DHRS2, and down regulation of HSP10, PGAM-B, RPS12, PSME-3, and TPT1 were reported for the first time in this study. In addition, we confirmed the regulation of mRNA expression levels by q-RT-PCR for the significantly regulated proteins by PTS. Among all the regulated proteins, NQO2 showed significant change in its fold expression after PTS treatment when compared with the control cells.

NAD(P)H dehydrogenase, quinone oxidoreductase, NQO2 belongs to the category of phase II detoxification enzymes that catalyze the formation of hydroquinones leading to the detoxification of toxins and plays a major role in evading ROS generation thereby protecting the cells from oxidative damage.[28] It plays a vital role in controlling the factors that mediate cell growth, differentiation, proliferation, and apoptosis.[29] It is also reported to play a major role in the prevention of malignancy through its participation in controlling cell number and size, coupling of signaling pathways, and modulation of p53.[30] In this present study, HepG2 cells express minimal level of NQO2 at basal conditions, whereas the PTS treatment upregulates this protein, which may be involved in cell death. In another study, resveratrol treatment in the prostate cancer cells induces NF-κB p65, mediated through NQO2.[30] Moreover, NQO2 contributes to the cell growth suppression by playing a role in the degradation of cyclin D1, which might also be a mechanism of PTS-induced apoptosis in HepG2 cells.[31]

Numerous studies have shown that VDAC plays an essential role in mammalian apoptosis and is a key functional target of Bcl-2 family of proteins.[32−34] VDAC1 binds with the Bcl-2 family of proteins and regulates its effects on apoptosis; interference with this interaction could facilitate apoptosis induction thereby enhancing the therapeutic potential of chemotherapeutic agents. It was further evidenced that quinones have been accounted to show increased anticancer activity by stimulating VDAC1 expression.[35]

In this study, upregulated VDAC1 protein level by PTS may function as a mediator of apoptosis by altering mitochondrial function. This was supported by the reports of Simamura et al. showing that the overexpression of VDAC1 in cancer cells resulted in the increased production of ROS thereby decreasing cell survival.[36] Scharstuhl et al. reported that curcumin induced fibroblast apoptosis through the release of apoptosis-inducing factor, which was mediated by VDAC1, Bax, facilitates Bax-VDAC interaction and also increased the expression of pro-apoptotic factor p53 leading to apoptosis.[37]

DHRS2, called Hep27 protein, widely expressed in normal cells and tissues was found to be localized in the nuclei, cytoplasm, and mitochondria.[38−40] It was identified as a nuclear cell-cycle regulated protein in cultured human hepatoblastoma cells and reported to quench the toxic effect of xenobiotics, and can inhibit p53 transcription and initiate its degradation.[41,42] In contrast, Hep27 has also been shown to play functional role in inhibiting cell proliferation and quiescence in many cancer types.[41,43] In the present study, the expression of DHRS2 was significantly increased by PTS treatment, which coincided with the study of Deisenroth et al. showing that translocation of this protein from the mitochondria to the nucleus and increase in its nuclear concentration promote p53 accumulation and stabilization leading to cell cycle arrest and apoptosis.[40,44]

HSP10 is known to form a heterodimer with HSP60, as part of the HSP60/10 protein folding machine, it exerts the function by capturing and refolding the proteins for its function and is known to act as a chaperone to maintain mitochondrial homeostasis.[45] HSP10 has been reported to be overexpresssed in several tumors including large bowel cancer and exocervical cancer, prostate cancer, and mantle cell lymphoma.[46−48] Overexpression of HSP10 in cancer cells has been shown to inhibit tumor cell apoptosis by increasing the abundance of antiapoptotic Bcl-2 and decreasing the expression of caspase-3, thus promoting tumor cell survival and angiogenesis. The increased level of HSP10 in the intracellular spaces was linked to pathogenesis in premalignant status; as a result, its up-regulation might serve as an index for early diagnosis.[47]In this study, the level of expression of HSP10 was decreased after PTS treatment, which may impair the protein folding machinery which initiates cancer cell death.

TPT1, an antiapoptotic protein also known as histamine-releasing factor (HRF) or p23, is ubiquitously expressed in normal and cancer cells and functions mainly in the cell cycle, mTOR pathway, apoptosis, and nuclear reprogramming.[48] TPT1 is accounted to play a role in tumor development and reported to inhibit the proapoptotic protein Bax from dimerizing in such a way that it prevents MAC (mitochondrial apoptosis-induced channel) pore formation. As a result, the flux of apoptotic factors into the cell gets inhibited.[49] Differential expression of TPT1 showed an induction of the immune response thereby promoting cancer.[50] In addition, TPT1 is an important regulator of p53 as its overexpression prevents apoptosis by destabilization of p53, which was demonstrated in human lung carcinoma cell line A549.[51] Little evidence demonstrated that down-regulation of TPT1 decreases tumor cell viability.[52] In this present study, the expression of TPT1 was significantly reduced by PTS treatment, and it might be one of the reasons for the induction of cell death.

PSME-3 is a proteasome activator which induces protein degradation by binding specifically to 20S proteasomes and stimulates the hydrolysis of peptides.[53] PSME-3 is an antiapoptotic factor and is shown to be involved in cancer progression and development.[54,55] It has been reported to be overexpressed in colorectal and thyroid cancer and play a role in all phases of carcinogenesis.[53,55] Anticancer therapy with the down regulation of PSME-3 can inhibit the proteasome leading to cell cycle arrest and induces apoptosis.[56] The increased expression of PSME-3 was found in HepG2 cells where the treatment with PTS significantly decreased the expression, and this may be due to the inhibition of the proteasome function. This observed result was correlated well with the study of Cheng et al. which showed that tetrandrine, an alkaloid compound, functions as a proteasome inhibitor and induces apoptosis in HepG2 cells.[57]

PGAM-B is a glycolytic enzyme known to be expressed in the liver, kidney, and brain and is shown to have a role in cancer cell metabolism and proliferation.[58,59] The down-regulation in PGAM-B expression was observed in PTS-treated HepG2 cells, which act as glycolysis inhibitors.[57] Moreover, Engel et al. showed that a peptide inhibitor of PGAM-B promotes growth arrest in tumor cell lines.[60] Modulation of this protein by

dx.doi.org/10.1021/tx5001392 | Chem. Res. Toxicol. XXXX, XXX, XXX−XXX

resveratrol in prostate cancer cells resulted in the arrest of the glycolytic pathway, which eventually leads to cell death.[58]

Most of the ribosomal proteins (RPs) are significantly conserved during evolution. RPs are known to be the functional center in the 30S ribosomal subunit, which is involved in protein synthesis. It stabilizes specific rRNA structures and promotes correct folding of rRNAs. Many RPs function as RNA chaperones, and few are reported to be associated with drug resistance.[61,62] Specific RPs have been shown to be expressed in an unbalanced manner in different carcinomas, and RPS12 was reported to be overexpressed in human squamous cell cervical, breast, and gastric, and also in colorectal cancers.[63,64] In this study, the increased expression of RPS12 was found in HepG2 cells. In turn, PTS treatment decreased the expression to a considerable fold. This result was similar to the tetrandrine treatment in HepG2 cells which showed a reduction in the expression levels of RPS12.

The accumulated data suggest that the mitochondria-mediated cell death pathway plays a vital role in triggering apoptosis in response to those stimuli. In this pathway, mitochondria undergoing permeability transition will release apoptosis-inducing factors from the mitochondrial intermembrane space into the cytosol to activate caspase-9, which in turn cleaves and activates executioner caspase-3. In the present study, the activities of caspase-3 were upregulated in PTS-treated HepG2 cells, indicating that caspases are involved in this apoptotic process. Bax is a key component for cell-induced apoptosis through mitochondrial stress.[65] Upon apoptotic stimulation, Bax forms oligomers and translocates from the cytosol to the mitochondrial membrane and has been demonstrated to induce cytochrome C release thereby initiating the cascade of apoptotic events.[66,67] HepG2 cells treated with PTS showed elevated levels of proapoptotic Bax expression, while antiapoptotic Bcl-2 was down-regulated after the significant increase of caspase-3 activity. On the basis of these findings, it is reasonable to conclude that in PTS-treated HepG2 cells, caspase and mitochondrial proteins played important roles in the activation of the apoptotic pathway.

In conclusion, the results of this present study emphasize the protein expression profile in HepG2 cells upon PTS treatment. It revealed the multiple PTS targets in which diverse regulation of different proteins resulted in apoptosis of HepG2 cells. This proteomic finding highlights the modulation of protein expression in HepG2 cells which might offer valuable insight into the mechanism of an antitumor effect of PTS. This may overlay a platform to exploit a new therapeutic candidate in cancer therapy.

■ ASSOCIATED CONTENT

Supporting Information

2-DE maps of control and PTS-treated HepG2 cells and differentially regulated protein spots. This material is available free of charge via the Internet at http://pubs.acs.org.

■ AUTHOR INFORMATION

Corresponding Author

*Tel: +91-9940737854. Fax: +91-44-2745 23437. E-mail: ramkumar.km@res.srmuniv.ac.in.

Funding

This work was supported by SRM University (to K.M.R.) and Stanford University (to R.P.).

Notes

The authors declare no competing financial interest.

■ ACKNOWLEDGMENTS

We thank Dr. Sanjiv Sam Gambhir, Chairman, Department of Radiology, and Canary Center at Stanford, for the facility.

■ ABBREVIATIONS

PTS, pterostilbene; HepG2, human hepatocellular liver carcinoma cell line; VDAC1, voltage-dependent anion-selective channel protein 1; NQO2, NAD(P)H dehydrogenase, quinone 2; DHRS2, dehydrogenase (reductase) SDR family member 2; HSP10, heat shock protein10; RPS12, 40S ribosomal protein S12; PGAM-B, phosphoglycerate mutase B; PSME-3, proteosome activator complex subunit 3; TPT1, translationally controlled tumor protein

■ REFERENCES

(1) Rimando, A. M., Kalt, W., Magee, J. B., Dewey, J., and Ballington, J. R. (2004) Resveratrol, pterostilbene, and piceatannol in vaccinium berries. *J. Agric. Food. Chem. 52*, 4713−4719.

(2) Hasiah, A. H., Ghazali, A. R., Weber, J. F., Velu, S., Thomas, N. F., and Inayat Hussain, S. H. (2011) Cytotoxic and antioxidant effects of methoxylated stilbene analogues on HepG2 hepatoma and Chang liver cells: Implications for structure activity relationship. *Hum. Exp. Toxicol. 30*, 138−144.

(3) Kapetanovic, I. M., Muzzio, M., Huang, Z., Thompson, T. N., and McCormick, D. L. (2011) Pharmacokinetics, oral bioavailability, and metabolic profile of resveratrol and its dimethylether analog, pterostilbene, in rats. *Cancer Chemother. Pharmacol. 68*, 593−601.

(4) McCormack, D., and McFadden, D. (2012) Pterostilbene and cancer: current review. *J. Surg. Res. 173*, e53−61.

(5) Pan, M. H., Chang, Y. H., Badmaev, V., Nagabhushanam, K., and Ho, C. T. (2007) Pterostilbene induces apoptosis and cell cycle arrest in human gastric carcinoma cells. *J. Agric. Food Chem. 55*, 7777−7785.

(6) Pan, M. H., Chiou, Y. S., Chen, W. J., Wang, J. M., Badmaev, V., and Ho, C. T. (2009) Pterostilbene inhibited tumor invasion via suppressing multiple signal transduction pathways in human hepatocellular carcinoma cells. *Carcinogenesis 30*, 1234−1242.

(7) Ghazali, A. R., Ki, O. S., Hamid, H. A., Room, N. M., and Kamarulzaman, F. (2012) Effect of psterostilbene on O-deethylation and glutathione conjugation of drug metabolizing enzyme activities. *Pharmacologia 3*, 456−461.

(8) Rubporn, A., Srisomsap, C., Subhasitanont, P., Chokchaichamnankit, D., Chiablaem, K., Svasti, J., and Sangvanich, P. (2009) Comparative proteomic analysis of lung cancer cell line and lung fibroblast cell line. *Cancer Genomics Proteomics 6*, 229−237.

(9) Aka, J. A., and Lin, S. X. (2012) Comparison of functional proteomic analyses of human breast cancer cell lines T47D and MCF7. *PLoS One 7*, e31532.

(10) Essid, E., and Petzinger, E. (2011) Silibinin pretreatment protects against ochratoxin A-mediated apoptosis in primary rat hepatocytes. *Mycotoxin Res. 27*, 167−176.

(11) Zhang, Y., and Zhao, B. (2003) Green tea polyphenols enhance sodium nitroprusside-induced neurotoxicity in human neuroblastoma SH-SY5Y cells. *J. Neurochem. 86*, 1189−1200.

(12) Gordaliza, M. (2007) Natural products as leads to anticancer drugs. *Clin. Transl. Oncol. 9*, 767−776.

(13) Castillo-Pichardo, L., and Dharmawardhane, S. F. (2012) Grape polyphenols inhibit Akt/mammalian target of rapamycin signaling and potentiate the effects of gefitinib in breast cancer. *Nutr. Cancer 64*, 1058−1069.

(14) Lambert, J. D., Hong, J., Yang, G. Y., Liao, J., and Yang, C. S. (2005) Inhibition of carcinogenesis by polyphenols: evidence from laboratory investigations. *Am. J. Clin. Nutr. 81*, 284S−291S.

(15) Ramos, S., Alia, M., Bravo, L., and Goya, L. (2005) Comparative effects of food-derived polyphenols on the viability and apoptosis of a

human hepatoma cell line (HepG2). *J. Agric. Food Chem. 53*, 1271−1280.
(16) Mannal, P. W., Alosi, J. A., Schneider, J. G., McDonald, D. E., and McFadden, D. W. (2010) Pterostilbene inhibits pancreatic cancer in vitro. *J. Gastrointest. Surg. 14*, 873−879.
(17) Hensley, K., Robinson, K. A., Gabbita, S. P., Salsman, S., and Floyd, R. A. (2000) Reactive oxygen species, cell signaling, and cell injury. *Free Radical Biol. Med. 28*, 1456−1462.
(18) Chang, Y. F., Chi, C. W., and Wang, J. J. (2006) Reactive oxygen species production is involved in quercetin-induced apoptosis in human hepatoma cells. *Nutr. Cancer 55*, 201−209.
(19) Kroemer, G., Galluzzi, L., and Brenner, C. (2007) Mitochondrial membrane permeabilization in cell death. *Physiol. Rev. 87*, 99−163.
(20) Alosi, J. A., McDonald, D. E., Schneider, J. S., Privette, A. R., and McFadden, D. W. (2010) Pterostilbene inhibits breast cancer in vitro through mitochondrial depolarization and induction of caspase-dependent apoptosis. *J. Surg. Res. 161*, 195−201.
(21) Mena, S., Rodriguez, M. L., Ponsoda, X., Estrela, J. M., Jaattela, M., and Ortega, A. L. (2012) Pterostilbene-induced tumor cytotoxicity: a lysosomal membrane permeabilization-dependent mechanism. *PLoS One 7*, e44524.
(22) Chiou, Y. S., Tsai, M. L., Nagabhushanam, K., Wang, Y. J., Wu, C. H., Ho, C. T., and Pan, M. H. (2011) Pterostilbene is more potent than resveratrol in preventing azoxymethane (AOM)-induced colon tumorigenesis via activation of the NF-E2-related factor 2 (Nrf2)-mediated antioxidant signaling pathway. *J. Agric. Food Chem. 59*, 2725−2733.
(23) Khan, M., Rasul, A., Yi, F., Zhong, L., and Ma, T. (2011) Jaceosidin induces p53-dependent G2/M phase arrest in U87 glioblastoma cells. *Asian Pac. J. Cancer Prev. 12*, 3235−3238.
(24) Naowaratwattana, W., De-Eknamkul, W., and De Mejia, E. G. (2010) Phenolic-containing organic extracts of mulberry (*Morus alba* L.) leaves inhibit HepG2 hepatoma cells through G2/M phase arrest, induction of apoptosis, and inhibition of topoisomerase IIalpha activity. *J. Med. Food 13*, 1045−1056.
(25) Lee, D. S., Lee, M. K., and Kim, J. H. (2009) Curcumin induces cell cycle arrest and apoptosis in human osteosarcoma (HOS) cells. *Anticancer Res. 29*, 5039−5044.
(26) Auyeung, K. K., and Ko, J. K. (2010) Novel herbal flavonoids promote apoptosis but differentially induce cell cycle arrest in human colon cancer cell. *Invest. New Drugs 28*, 1−13.
(27) Simpson, R. J., and Dorow, D. S. (2001) Cancer proteomics: from signaling networks to tumor markers. *Trends Biotechnol. 19*, S40−48.
(28) Ross, D., and Siegel, D. (2004) NAD(P)H:quinone oxidoreductase 1 (NQO1, DT-diaphorase), functions and pharmacogenetics. *Methods Enzymol. 382*, 115−144.
(29) Shen, J., Barrios, R. J., and Jaiswal, A. K. (2010) Inactivation of the quinone oxidoreductases NQO1 and NQO2 strongly elevates the incidence and multiplicity of chemically induced skin tumors. *Cancer Res. 70*, 1006−1014.
(30) Hsieh, T. C. (2009) Antiproliferative effects of resveratrol and the mediating role of resveratrol targeting protein NQO2 in androgen receptor-positive, hormone-non-responsive CWR22Rv1 cells. *Anticancer Res. 29*, 3011−3017.
(31) Hsieh, T. C., Yang, C. J., Lin, C. Y., Lee, Y. S., and Wu, J. M. (2012) Control of stability of cyclin D1 by quinone reductase 2 in CWR22Rv1 prostate cancer cells. *Carcinogenesis 33*, 670−677.
(32) Simamura, E., Hirai, K., Shimada, H., Koyama, J., Niwa, Y., and Shimizu, S. (2006) Furanonaphthoquinones cause apoptosis of cancer cells by inducing the production of reactive oxygen species by the mitochondrial voltage-dependent anion channel. *Cancer Biol. Ther. 5*, 1523−1529.
(33) Arbel, N., and Shoshan-Barmatz, V. (2010) Voltage-dependent anion channel 1-based peptides interact with Bcl-2 to prevent antiapoptotic activity. *J. Biol. Chem. 285*, 6053−6062.
(34) Tajeddine, N., Galluzzi, L., Kepp, O., Hangen, E., Morselli, E., Senovilla, L., Araujo, N., Pinna, G., Larochette, N., Zamzami, N., Modjtahedi, N., Harel-Bellan, A., and Kroemer, G. (2008) Hierarchical involvement of Bak, VDAC1 and Bax in cisplatin-induced cell death. *Oncogene 27*, 4221−4232.
(35) Simamura, E., Shimada, H., Ishigaki, Y., Hatta, T., Higashi, N., and Hirai, K. (2008) Bioreductive activation of quinone antitumor drugs by mitochondrial voltage-dependent anion channel 1. *Anat. Sci. Int. 83*, 261−266.
(36) Simamura, E., Shimada, H., Hatta, T., and Hirai, K. (2008) Mitochondrial voltage-dependent anion channels (VDACs) as novel pharmacological targets for anti-cancer agents. *J. Bioenerg. Biomembr. 40*, 213−217.
(37) Scharstuhl, A., Mutsaers, H. A., Pennings, S. W., Russel, F. G., and Wagener, F. A. (2009) Involvement of VDAC, Bax and ceramides in the efflux of AIF from mitochondria during curcumin-induced apoptosis. *PLoS One 4*, e6688.
(38) Heinz, S., Krause, S. W., Gabrielli, F., Wagner, H. M., Andreesen, R., and Rehli, M. (2002) Genomic organization of the human gene HEP27: alternative promoter usage in HepG2 cells and monocyte-derived dendritic cells. *Genomics 79*, 608−615.
(39) Shafqat, N., Shafqat, J., Eissner, G., Marschall, H. U., Tryggvason, K., Eriksson, U., Gabrielli, F., Lardy, H., Jornvall, H., and Oppermann, U. (2006) Hep27, a member of the short-chain dehydrogenase/reductase family, is an NADPH-dependent dicarbonyl reductase expressed in vascular endothelial tissue. *Cell. Mol. Life Sci. 63*, 1205−1213.
(40) Deisenroth, C., Thorner, A. R., Enomoto, T., Perou, C. M., and Zhang, Y. (2010) Mitochondrial Hep27 is a c-Myb target gene that inhibits Mdm2 and stabilizes p53. *Mol. Cell. Biol. 30*, 3981−3993.
(41) Gabrielli, F., Donadel, G., Bensi, G., Heguy, A., and Melli, M. (1995) A nuclear protein, synthesized in growth-arrested human hepatoblastoma cells, is a novel member of the short-chain alcohol dehydrogenase family. *Eur. J. Biochem. 232*, 473−477.
(42) Monge, M., Colas, E., Doll, A., Gil-Moreno, A., Castellvi, J., Diaz, B., Gonzalez, M., Lopez-Lopez, R., Xercavins, J., Carreras, R., Alameda, F., Canals, F., Gabrielli, F., Reventos, J., and Abal, M. (2009) Proteomic approach to ETV5 during endometrial carcinoma invasion reveals a link to oxidative stress. *Carcinogenesis 30*, 1288−1297.
(43) Petropavlovskaia, M., Bodnar, C. A., Behie, L. A., and Rosenberg, L. (2007) Pancreatic small cells: analysis of quiescence, long-term maintenance and insulin expression in vitro. *Exp. Cell. Res. 313*, 931−942.
(44) Thorner, A. R., Parker, J. S., Hoadley, K. A., and Perou, C. M. (2010) Potential tumor suppressor role for the c-Myb oncogene in luminal breast cancer. *PLoS One 5*, e13073.
(45) Czarnecka, A. M., Campanella, C., Zummo, G., and Cappello, F. (2006) Heat shock protein 10 and signal transduction: a "capsula eburnea" of carcinogenesis? *Cell Stress Chaperones 11*, 287−294.
(46) Ghobrial, I. M., McCormick, D. J., Kaufmann, S. H., Leontovich, A. A., Loegering, D. A., Dai, N. T., Krajnik, K. L., Stenson, M. J., Melhem, M. F., Novak, A. J., Ansell, S. M., and Witzig, T. E. (2005) Proteomic analysis of mantle-cell lymphoma by protein microarray. *Blood 105*, 3722−3730.
(47) Jia, H., Halilou, A. I., Hu, L., Cai, W., Liu, J., and Huang, B. (2011) Heat shock protein 10 (Hsp10) in immune-related diseases: one coin, two sides. *Int. J. Biochem. Mol. Biol. 2*, 47−57.
(48) Arcuri, F., Papa, S., Carducci, A., Romagnoli, R., Liberatori, S., Riparbelli, M. G., Sanchez, J. C., Tosi, P., and del Vecchio, M. T. (2004) Translationally controlled tumor protein (TCTP) in the human prostate and prostate cancer cells: expression, distribution, and calcium binding activity. *Prostate 60*, 130−140.
(49) Petros, A. M., Olejniczak, E. T., and Fesik, S. W. (2004) Structural biology of the Bcl-2 family of proteins. *Biochim. Biophys. Acta 1644*, 83−94.
(50) MacDonald, S. M., Rafnar, T., Langdon, J., and Lichtenstein, L. M. (1995) Molecular identification of an IgE-dependent histamine-releasing factor. *Science 269*, 688−690.
(51) Rho, S. B., Lee, J. H., Park, M. S., Byun, H. J., Kang, S., Seo, S. S., Kim, J. Y., and Park, S. Y. (2011) Anti-apoptotic protein TCTP controls the stability of the tumor suppressor p53. *FEBS Lett. 585*, 29−35.

(52) Tuynder, M., Fiucci, G., Prieur, S., Lespagnol, A., Geant, A., Beaucourt, S., Duflaut, D., Besse, S., Susini, L., Cavarelli, J., Moras, D., Amson, R., and Telerman, A. (2004) Translationally controlled tumor protein is a target of tumor reversion. *Proc. Natl. Acad. Sci. U.S.A. 101*, 15364−15369.
(53) Roessler, M., Rollinger, W., Mantovani-Endl, L., Hagmann, M. L., Palme, S., Berndt, P., Engel, A. M., Pfeffer, M., Karl, J., Bodenmuller, H., Ruschoff, J., Henkel, T., Rohr, G., Rossol, S., Rosch, W., Langen, H., Zolg, W., and Tacke, M. (2006) Identification of PSME3 as a novel serum tumor marker for colorectal cancer by combining two-dimensional polyacrylamide gel electrophoresis with a strictly mass spectrometry-based approach for data analysis. *Mol. Cell. Proteomics 5*, 2092−2101.
(54) Rechsteiner, M., and Hill, C. P. (2005) Mobilizing the proteolytic machine: cell biological roles of proteasome activators and inhibitors. *Trends Cell Biol. 15*, 27−33.
(55) Okamura, T., Taniguchi, S., Ohkura, T., Yoshida, A., Shimizu, H., Sakai, M., Maeta, H., Fukui, H., Ueta, Y., Hisatome, I., and Shigemasa, C. (2003) Abnormally high expression of proteasome activator-gamma in thyroid neoplasm. *J. Clin. Endocrinol. Metab.*, 1374−1383.
(56) Zhang, M., Gan, L., and Ren, G. S. (2012) REGgamma is a strong candidate for the regulation of cell cycle, proliferation and the invasion by poorly differentiated thyroid carcinoma cells. *Braz. J. Med. Biol. Res. 45*, 459−465.
(57) Cheng, Z., Wang, K., Wei, J., Lu, X., and Liu, B. (2010) Proteomic analysis of anti-tumor effects by tetrandrine treatment in HepG2 cells. *Phytomedicine 17*, 1000−1005.
(58) Narayanan, N. K., Narayanan, B. A., and Nixon, D. W. (2004) Resveratrol-induced cell growth inhibition and apoptosis is associated with modulation of phosphoglycerate mutase B in human prostate cancer cells: two-dimensional sodium dodecyl sulfate-polyacrylamide gel electrophoresis and mass spectrometry evaluation. *Cancer Detect. Prev. 28*, 443−452.
(59) Kondoh, H., Lleonart, M. E., Gil, J., Wang, J., Degan, P., Peters, G., Martinez, D., Carnero, A., and Beach, D. (2005) Glycolytic enzymes can modulate cellular life span. *Cancer Res. 65*, 177−185.
(60) Engel, M., Mazurek, S., Eigenbrodt, E., and Welter, C. (2004) Phosphoglycerate mutase-derived polypeptide inhibits glycolytic flux and induces cell growth arrest in tumor cell lines. *J. Biol. Chem. 279*, 35803−35812.
(61) Coukell, M. B., and Polglase, W. J. (1969) Relaxation of catabolite repression in streptomycin-dependent *Escherichia coli*. *Biochem. J. 111*, 279−286.
(62) Shen, D. W., Liang, X. J., Suzuki, T., and Gottesman, M. M. (2006) Identification by functional cloning from a retroviral cDNA library of cDNAs for ribosomal protein L36 and the 10-kDa heat shock protein that confer cisplatin resistance. *Mol. Pharmacol. 69*, 1383−1388.
(63) Deng, S. S., Xing, T. Y., Zhou, H. Y., Xiong, R. H., Lu, Y. G., Wen, B., Liu, S. Q., and Yang, H. J. (2006) Comparative proteome analysis of breast cancer and adjacent normal breast tissues in human. *Genomics, Proteomics Bioinf. 4*, 165−172.
(64) Pogue-Geile, K., Geiser, J. R., Shu, M., Miller, C., Wool, I. G., Meisler, A. I., and Pipas, J. M. (1991) Ribosomal protein genes are overexpressed in colorectal cancer: isolation of a cDNA clone encoding the human S3 ribosomal protein. *Mol. Cell. Biol. 11*, 3842−3849.
(65) Theodorakis, P., Lomonosova, E., and Chinnadurai, G. (2002) Critical requirement of BAX for manifestation of apoptosis induced by multiple stimuli in human epithelial cancer cells. *Cancer Res. 62*, 3373−3376.
(66) Marzo, I., Brenner, C., Zamzami, N., Jurgensmeier, J. M., Susin, S. A., Vieira, H. L., Prevost, M. C., Xie, Z., Matsuyama, S., Reed, J. C., and Kroemer, G. (1998) Bax and adenine nucleotide translocator cooperate in the mitochondrial control of apoptosis. *Science 281*, 2027−2031.
(67) Lakhani, S. A., Masud, A., Kuida, K., Porter, G. A., Jr., Booth, C. J., Mehal, W. Z., Inayat, I., and Flavell, R. A. (2006) Caspases 3 and 7: key mediators of mitochondrial events of apoptosis. *Science 311*, 847−851.